

Exclusive Double Diffractive Events: general framework and prospects

R.A. Ryutin^{a1}

Institute for High Energy Physics, 142 281, Protvino, Russia

Abstract. We consider the general theoretical framework to study exclusive double diffractive events (EDDE). It is a powerful tool to explore the picture of the pp interaction. Basic kinematical and dynamical properties of the process, and also normalization of parameters via standard processes like the exclusive vector meson production (EVMP), are considered in detail. As an example, calculations of the cross-sections in the model with three pomerons for the process $p + p \rightarrow p + M + p$ are presented for Tevatron and LHC energies.

PACS. 11.55.Jy Regge formalism – 12.38.Bx Perturbative calculations – 12.40.Nn Regge theory, duality, absorptive/optical models – 12.39.Jh Nonrelativistic quark model – 13.85.Ni Inclusive production with identified hadrons

1 Introduction

Impressive progress of the LHC experiments stimulates new investigations in different areas of high energy physics. Latest weighty arguments in favor of the existence of the Higgs boson give us the basis for further experiments, since we have to define exactly the nature of this particle. It is a problem of today to have a clear instrument to determine its quantum numbers and couplings to other particles. Besides this task concerning Higgs boson, we have to continue to study other fundamental objects of high energy physics like jets and particles produced in different processes.

If we consider huge number of high energy processes which have been studied for a long time, we will find the one which can serve as a clear source of information about high-energy dynamics. It is the exclusive double diffractive event (EDDE), i.e. the process of the type $h + h \rightarrow h^* + M + h^*$, where $h \rightarrow h^*$ scattering is quasi-diffractive, M is the centrally produced particle or system of particles and “+” means large rapidity gap (LRG). If one takes M as a single particle produced, this is the first “genuinely” inelastic process which not only retains a lot of features of elastic scattering (diffractive patterns), but also shows clearly how the initial energy is being transformed into the secondary particles. General properties of such amplitudes were considered in Ref. [1]-[3]. Theoretical consideration of these processes on the basis of Regge theory goes back to papers [4]-[9]. The recent interest is related to possibly good signals of centrally produced Higgs

bosons, heavy quarkonia, glueballs, jets, gauge bosons, system of hadrons [10]-[30].

Experimental study has begun since 1970’s [31]. As Pomeron are the driving force of the processes in question at high energies it is naturally to expect that glueball production will be favorable, if one believes that Pomerons are mostly gluonic objects. Central glueball production was suggested as possible origin of the total cross section rise in Ref. [3]. One of the early proposal for experimental investigations of centrally produced glueballs in EDDE was made in [32]. As to the most recent experimental studies one has to mention the series of results from the experiment WA102 [33]-[37]. With energy rise we can observe central systems with higher masses [38], like di-jet [39], di-gamma [40],[41],[42], heavy quarkonia [44], di-hadron ([45] and references therein).

EDDE gives us unique experimental possibilities for particle searches and investigations of diffraction proper. This is due to several advantages of the process:

- clear signature of the process: central system separated from two finally detected protons by LRGs (see, for example, theoretical work [48], the experimental one [49] and references therein);
- possibility to use the “missing mass method” [50] that improves the mass resolution;
- strong suppression of the background due to the $J_z = 0$ selection rule [51]-[53] for basic processes like, for example, Higgs boson production;
- spin-parity analysis of the central system can be done to determine quantum numbers of the central particle [54]-[59];

^a e-mail: Roman.Rioutine@cern.ch

- interesting measurements concerning the interplay between “soft” and “hard” scales are possible: we can obtain basic features of the interaction region (size and shape) from distributions in the scattering angle (diffractive patterns) [15].

There are several proposals to realize the above properties at LHC [60]-[62]. Due to the complicated picture of the interaction at high luminosities (a lot of “pile-up” events) at the moment we only have the possibility to select EDDE without detection of final protons [63],[42]. The criterium of LRGs is not sufficient for our investigations, since we lose basic advantages of the exclusive process. For the experiment we need special low luminosity runs. In fact, latest LHC experiments show that the definition of diffraction is rather complicated subject [64], which needs further investigations.

A new physics program based on polarized proton beams and tagging of forward protons has been launched also at STAR/RHIC [65]-[68]. These experiments can drastically improve our understanding of diffractive mechanisms and suppress uncertainties that can reach sometimes an order of magnitude.

There are many theoretical groups now that work in this area [10]-[30]. All these models need to obtain values of their parameters to make predictions for the LHC energies. For this purpose we can use so called “standard candle” processes, i.e. events which have the same theoretical ingredients for the calculations. Usually authors use the following processes:

for high central masses ($M \gg 1$ GeV, perturbative mechanism of Pomeron-Pomeron fusion dominates)

- $\gamma^* + p \rightarrow V + p$ (Exclusive Vector Meson Production, EVMP), $m_V \gg 1$ GeV [69]-[71];
- $p + p \rightarrow p + M + p$, $M = jj$ [39], $M = \gamma\gamma$ [40],[41],[42], $M = \{Q\bar{Q}\}$ (heavy quarkonia, $\chi_{c,b}$) [44], $M = hh$ (dihadron system) [45];

for low central masses ($M \sim 1$ GeV, nonperturbative Pomeron-Pomeron fusion)

- $\gamma^* + p \rightarrow V + p$ (EVMP), $m_V \sim 1$ GeV [72]-[74];
- $p + p \rightarrow p + M + p$, $M = \{q\bar{q}\}$ (light meson) or “glueball” [33]-[37], $M = hh$ (dihadron system) [45];

In the low-mass case the mechanism of Pomeron-Pomeron fusion is considerably nonperturbative. It will be taken into account in the calculations.

In this paper we try to consider a general model-independent framework for EDDE. Our model for diffractive processes is taken as an example.

2 Exclusive vector meson photoproduction.

In this chapter we consider EVMP, i.e. exclusive photoproduction of $V = Q\bar{Q}_{1S}$ states, as the first “standard candle” for the EDDE. It was considered in [46] in the framework of the three Pomeron model [47]. Here we present a more general situation and correct formulae for parameters and integrals. Basic ingredients of the theoretical framework

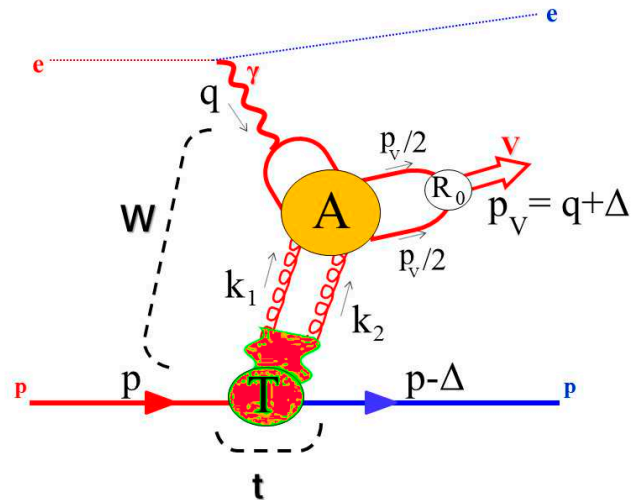


Fig. 1. Exclusive vector meson photoproduction in the NRQCD framework. W is the γp collision energy. $t = -\Delta^2$ is the transferred momentum squared. Directions of momenta are shown by arrows. Vertices A , T and R_0 are defined in the text.

are presented in the Fig. 1 and in subsections 2.1-2.3. Below we consider perturbative mechanism of EVMP, i.e. the mass of a vector meson is much greater than 1 GeV in this case. Nonperturbative mechanisms (see Fig. 11) will be presented in further works. Following the scheme depicted in the Fig. 1 we can write the amplitude of the process as a convolution of the diffractive gluon-proton amplitude T and perturbative amplitude A , which is considered in an appropriate approach.

2.1 Kinematics.

First, let us introduce the notations for four-vectors depicted in the Fig. 1. For any four-vector we use two following representations,

$$\begin{aligned} \text{usual: } v &= (v_0, v_3; \mathbf{v}_t) \\ \text{and "light-cone": } v &= \{v_+, v_-; \mathbf{v}_t\}. \end{aligned} \quad (1)$$

For external vectors we have:

$$p = \left(\frac{W^2 + Q^2 + m^2}{2W}, \frac{\lambda^{1/2}(W^2, m^2, -Q^2)}{2W}; \mathbf{0} \right), \quad (2)$$

$$q = \left(\frac{W^2 - Q^2 - m^2}{2W}, -\frac{\lambda^{1/2}(W^2, m^2, -Q^2)}{2W}; \mathbf{0} \right), \quad (3)$$

$$\Delta_3 = \frac{W^2(m_V^2 + Q^2 - 3t) + (m^2 + Q^2)(m_V^2 + Q^2 + t)}{2\lambda^{1/2}(W^2, m^2, -Q^2)W},$$

$$\Delta = \left(\frac{m_V^2 + Q^2 + t}{2W}, \Delta_3; \mathbf{\Delta} \right), \quad (4)$$

where

$$\lambda(x, y, z) = x^2 + y^2 + z^2 - 2xy - 2xz - 2yz, \quad (5)$$

$$s = W^2, \quad q^2 = -Q^2, \quad p^2 = m^2, \quad \Delta^2 = t, \quad p_V^2 = m_V^2. \quad (6)$$

Let us introduce some basic variables:

$$\begin{aligned}
k_1 &= \kappa + \frac{\Delta}{2}, \quad k_2 = -\kappa + \frac{\Delta}{2}, \\
p' &= p - \frac{m^2}{\tilde{s}}q, \quad q' = q + \frac{Q^2}{\tilde{s}}p, \quad p_V = q + \Delta, \\
q'^2 &= p'^2 = 0, \quad \tilde{s} = pq + \sqrt{(pq)^2 + Q^2 m^2}, \\
\kappa &= \frac{z_v}{2}(y_+ p' + y_- q') + \kappa_\perp, \\
\Delta &= z_v^2 ([1 + y_Q + y_\Delta] p' - y_\Delta q') + \Delta_\perp, \\
z_v &= \frac{m_V}{W}, \quad y = -\frac{4\kappa^2}{m_V^2}, \quad y_Q = \frac{Q^2}{m_V^2}, \\
t &\simeq \Delta_\perp^2 = -\Delta^2, \quad y_\Delta = \frac{\Delta^2}{m_V^2}, \quad y_0 = \frac{4s_0}{m_V^2}, \\
\kappa_\perp^2 &= -\kappa^2 = -\frac{m_V^2}{4} \left(y + 4y_+ y_- \frac{2p' q'}{W^2} \right) \\
&\simeq -\frac{m_V^2}{4} (y + 4y_+ y_-), \tag{7}
\end{aligned}$$

$s_0 = 1 \text{ GeV}^2$.

Photon and vector meson polarization vectors in the general case ($Q \neq 0$) can be represented as follows:

$$\begin{aligned}
\epsilon_{\gamma_\perp} q &= \epsilon_{\gamma_0} q = 0, \quad \epsilon_{\gamma_\perp}^2 = -\epsilon_{\gamma_0}^2 = -1, \\
\epsilon_{\gamma_0} &= \frac{1}{Q}(q' + z_v^2 y_Q p'), \\
\epsilon_{V_\perp} p_V &= \epsilon_{V_\parallel} p_V = 0, \\
\epsilon_{V_\perp} &= v_\perp + \frac{2(v_\Delta)}{s}(p' - q'), \quad v_\perp^2 = -v^2, \\
\epsilon_{V_\parallel} &= \frac{1}{m_V}(q' - z_v^2(1 - y_\Delta)p' + \Delta_\perp) \tag{8}
\end{aligned}$$

For high-energy photoproduction ($Q \rightarrow 0$) we have

$$\begin{aligned}
Q &\ll m, \quad m_V, \quad \sqrt{-t} \ll W, \\
z_m &= \frac{m}{W}, \quad z_Q = \frac{Q}{W}, \quad z_t = \frac{\sqrt{-t}}{W}, \\
k_1 &\simeq \left\{ \frac{W}{\sqrt{2}} z_v \left(y_+ + \frac{z_v}{2} \right), \frac{W}{\sqrt{2}} z_v y_-; \kappa \right\}, \\
k_2 &\simeq \left\{ -\frac{W}{\sqrt{2}} z_v \left(y_+ - \frac{z_v}{2} \right), -\frac{W}{\sqrt{2}} z_v y_-; -\kappa \right\}, \\
p_V &\simeq \left\{ \frac{W}{\sqrt{2}} (z_v^2 + z_t^2), \frac{W}{\sqrt{2}}; \sqrt{-t} \frac{\Delta}{|\Delta|} \right\}, \\
p &\simeq p' \simeq \left\{ \frac{W}{\sqrt{2}}, 0; \mathbf{0} \right\}, \quad q \simeq q' \simeq \left\{ 0, \frac{W}{\sqrt{2}}, \mathbf{0} \right\}. \tag{9}
\end{aligned}$$

It is convenient to introduce two transverse polarization vectors

$$\begin{aligned}
\epsilon_1 &= (0, 0; (1, 0)), \quad \epsilon_2 = (0, 0; (0, 1)), \\
\epsilon_i &\perp p, q, p_V, \quad \epsilon_i^2 = -1, \\
\epsilon_i k_1 &= -\epsilon_i k_2 = \epsilon_i \kappa = - \begin{cases} \kappa_t \cos \phi \\ \kappa_t \sin \phi \end{cases} \tag{10}
\end{aligned}$$

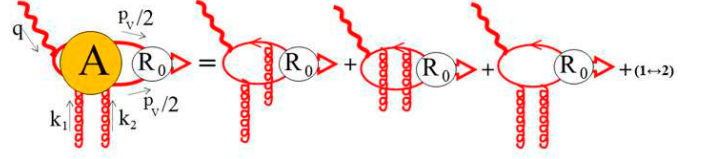


Fig. 2. Exclusive vector meson photoproduction in the NRQCD framework. Hard amplitude.

2.2 Soft and hard amplitudes.

2.2.1 NRQCD framework for the hard part of the amplitude.

The amplitude A of the process $\gamma(q) + g(k_1) \rightarrow V(p_V) + g(-k_2)$ (Fig. 2) is calculated in the nonrelativistic bound state approximation (see [75]-[77] and ref. therein):

$$\begin{aligned}
\tilde{O}_{\epsilon_\gamma, \epsilon_V}^{\alpha\beta} &= Sp \left[\hat{O}^{\alpha\beta} (\hat{p}_V - m_V) \hat{\epsilon}_V \right], \quad \mathcal{K}_V = \frac{8R_{V,0} \pi e_Q \sqrt{\alpha_e} \alpha_s}{\sqrt{3} m_V}, \\
A^{\text{ab}, \alpha\beta} &= \frac{R_{V,0}}{4\sqrt{\pi} m_V} \times e_Q \sqrt{4\pi} \alpha_e \times 4\pi \alpha_s \times \left[t_{ij}^a t_{jk}^b \frac{\delta^{ik}}{\sqrt{3}} \right] \tilde{O}_{\epsilon_\gamma, \epsilon_V}^{\alpha\beta} \\
&= \mathcal{K}_V \frac{\delta^{\text{ab}}}{8} \tilde{O}_{\epsilon_\gamma, \epsilon_V}^{\alpha\beta}, \tag{11}
\end{aligned}$$

where e_Q is the charge of heavy quark Q , $R_{V,0}$ is the absolute value of the vector meson radial wave function at the origin, $\left[t_{ij}^a t_{jk}^b \frac{\delta^{ik}}{\sqrt{3}} \right] = \frac{\delta^{\text{ab}}}{2\sqrt{3}}$ due to SU(3) group rules and

$$\begin{aligned}
\hat{O}^{\alpha\beta} &= \left\{ \frac{\gamma^\alpha \left(-\hat{k}_1 + \frac{\hat{p}_V + m_V}{2} \right) \hat{\epsilon}_\gamma \left(\hat{k}_2 + \frac{-\hat{p}_V + m_V}{2} \right) \gamma^\beta}{(-p_V k_1 + k_1^2 + i0) (-p_V k_2 + k_2^2 + i0)} \right. \\
&\quad + \frac{\epsilon_\gamma \left(\hat{k}_1 + \hat{k}_2 + \frac{-\hat{p}_V + m_V}{2} \right) \gamma^\alpha \left(\hat{k}_2 + \frac{-\hat{p}_V + m_V}{2} \right) \gamma^\beta}{(-p_V(k_1 + k_2) + (k_1 + k_2)^2 + i0) (-p_V k_2 + k_2^2 + i0)} \\
&\quad \left. + \frac{\gamma^\alpha \left(-\hat{k}_1 + \frac{\hat{p}_V + m_V}{2} \right) \gamma^\beta \left(-\hat{k}_1 - \hat{k}_2 + \frac{\hat{p}_V + m_V}{2} \right) \hat{\epsilon}_\gamma}{(-p_V k_1 + k_1^2 + i0) (-p_V(k_1 + k_2) + (k_1 + k_2)^2 + i0)} \right\} \\
&\quad + (1 \leftrightarrow 2). \tag{12}
\end{aligned}$$

After calculations we have

$$\begin{aligned}
\tilde{O}_{\epsilon_\gamma, \epsilon_V}^{\alpha\beta} &= -16m_V \left\{ k_1 k_2 \right. \\
&\quad \times \left[p_V^\alpha \left(\epsilon_V^\beta k_2 \epsilon_\gamma - \epsilon_\gamma^\beta k_2 \epsilon_V \right) + p_V^\beta \left(\epsilon_V^\alpha k_1 \epsilon_\gamma - \epsilon_\gamma^\alpha k_1 \epsilon_V \right) \right] \\
&\quad + \left(\epsilon_V^\alpha \epsilon_\gamma^\beta k_1 k_2 + g^{\alpha\beta} k_1 \epsilon_V k_2 \epsilon_\gamma \right) (k_1^2 - k_1 p_V + k_1 k_2) \\
&\quad + \left(\epsilon_V^\beta \epsilon_\gamma^\alpha k_1 k_2 + g^{\alpha\beta} k_2 \epsilon_V k_1 \epsilon_\gamma \right) (k_2^2 - k_2 p_V + k_1 k_2) - \epsilon_V \epsilon_\gamma \\
&\quad \times \left[g^{\alpha\beta} (k_1^2 - k_1 p_V + k_1 k_2) (k_2^2 - k_2 p_V + k_1 k_2) + p_V^\alpha p_V^\beta k_1 k_2 \right] \\
&\quad \times \left[(-p_V k_1 + k_1^2 + i0) (-p_V k_2 + k_2^2 + i0) \right. \\
&\quad \left. (-p_V(k_1 + k_2) + (k_1 + k_2)^2 + i0) \right]^{-1}. \tag{13}
\end{aligned}$$

2.2.2 Diffractive part of the amplitude.

Diffractive gluon-proton amplitude can be written as

$$\begin{aligned} T^{\text{ab}, \alpha\beta} &\equiv T^{\text{ab}, \alpha\beta}(p, k_1, k_2) \\ &= \delta^{\text{ab}} \tilde{G}^{\alpha\beta}(p, k_1, k_2) T^D((p - k_1)^2, t, k_1 k_2), \end{aligned} \quad (14)$$

where

$$\begin{aligned} \tilde{G}^{\alpha\beta} &= G^{\alpha\beta} - \frac{P_1^\alpha P_2^\beta}{P_1 P_2}, \\ G^{\alpha\beta} &= g^{\alpha\beta} - \frac{k_2^\alpha k_1^\beta}{k_1 k_2}, \quad P_{1,2} = p - k_{2,1} \frac{p k_{1,2}}{k_1 k_2}. \end{aligned} \quad (15)$$

Strictly speaking, in the general case we have to write more than one transverse tensor structures, but in most cases these structures satisfy relations like the Callan-Gross one [78],[79]. Here we can neglect terms of the order $o(t)$ and $o(z_v^2)$. Further we will take into account relations

$$k_{1, \alpha} T^{\text{ab}, \alpha\beta} = 0, \quad k_{2, \beta} T^{\text{ab}, \alpha\beta} = 0, \quad (16)$$

that allow us to replace the tensor part of gluon propagators by metric tensors.

Let us denote

$$\mathcal{T}_{\epsilon_\gamma, \epsilon_V} = \tilde{O}_{\epsilon_\gamma, \epsilon_V}^{\alpha\beta} d_{\alpha\alpha'} d_{\beta\beta'} \tilde{G}^{\alpha'\beta'}, \quad (17)$$

where

$$\begin{aligned} d_{\alpha\alpha'} &= -g^{\alpha\alpha'} + \frac{1}{(k_1 k_2)^2 - k_1^2 k_2^2} \\ &\times [k_1 k_2 (k_{1, \alpha} k_{2, \alpha'} + k_1, \alpha' k_2, \alpha) \\ &- k_1^2 k_{2, \alpha} k_{2, \alpha'} - k_2^2 k_{1, \alpha} k_{1, \alpha'}] \end{aligned} \quad (18)$$

is the tensor part of the gluon propagator in the axial gauge with the axial vector $n = k_1 + k_2 = \Delta$ and

$$\Delta \rightarrow 0 \implies t \rightarrow 0 \implies n^2 \rightarrow 0.$$

We can obtain the main (diagonal) contribution for further calculations when we set $\epsilon_\gamma = \epsilon_V = \epsilon_i$ ($i = 1, 2$)

$$\begin{aligned} \mathcal{T}_{(i,i)} &= \frac{8f_c(y, y_+, y_-)}{m_V (y_-^2 + z_m^2 y)} \\ &\times \frac{1}{(y_+ - \frac{z_v}{2}(1+y) + i0)(y_+ + \frac{z_v}{2}(1+y) - i0)}, \quad (19) \\ f_c(y, y_+, y_-) &= y^2 - 2z_v^2 y_-^2 (1 + (1 + 2c^2)y) \\ &+ 4y_- y_+ (y - 4c^2 z_v^2 y_-^2) + 8y_-^2 y_+^2. \end{aligned} \quad (20)$$

In the above equation (20) c is the corresponding trigonometric function $\cos \phi$ ($i = 1$) or $\sin \phi$ ($i = 2$). In the next subsection we will have to take the integral over ϕ , which is equivalent to the replacement $c^2 \rightarrow 1/2$ that is why it is convenient to introduce the following function

$$\begin{aligned} f(y, y_+, y_-) &= \int_0^\pi \frac{d\phi}{\pi} f_c(y, y_+, y_-) \\ &= y^2 - 2z_v^2 y_-^2 (1 + 2y) + 4y_- y_+ (y - 2z_v^2 y_-^2) + 8y_-^2 y_+^2. \end{aligned} \quad (21)$$

2.2.3 Convolution and integration. Extraction of parameters for the diffractive amplitude.

After all convolutions the diagonal element of the amplitude for the process $\gamma + p \rightarrow V + p$ looks as follows

$$\begin{aligned} \mathcal{M}_{i,i} &= \int \frac{d^4 \kappa}{(2\pi)^4} \mathcal{K}_V \mathcal{T}_{(i,i)} T^D((p - k_1)^2) \\ &= \int dy dy_+ dy_- \int_0^\pi \frac{d\phi}{\pi} \frac{\pi m_V^4}{8} \frac{\mathcal{K}_V \mathcal{T}_{(i,i)} T^D(z_v y - s)}{(2\pi)^4} \\ &\times \left[\frac{4}{m_V^4 z_v^2 (y_-^2 - (\tilde{y}_- - i0)^2)} \right] \\ &= \bar{\mathcal{K}}_V \mathcal{I}_V \end{aligned} \quad (22)$$

$$\begin{aligned} \mathcal{I}_V &= \frac{1}{8} \int dy dy_+ dy_- \frac{f(y, y_+, y_-)}{z_v^2 (y_-^2 + z_m^2 y)} \\ &\times \frac{T^D(z_v y - s)}{(y_-^2 - (\tilde{y}_- - i0)^2) (y_+^2 - (\tilde{y}_+ - i0)^2)}, \end{aligned} \quad (23)$$

$$\bar{\mathcal{K}}_V = \frac{16 R_{V,0} e_Q \sqrt{\alpha_e} \alpha_s}{\sqrt{3} m_V^{3/2} \pi^2}, \quad (24)$$

$$\tilde{y}_- = \left| \frac{y}{2z_v} \right|, \quad \tilde{y}_+ = \left| \frac{z_v}{2} (1 + y) \right|. \quad (25)$$

Integral (23) can be represented in the following form

$$\mathcal{I}_V \simeq \frac{1}{8} \int_0^1 dy \left\{ \tilde{f}_+ \hat{\mathcal{I}}_+ + \tilde{f}_- \hat{\mathcal{I}}_- \right\}, \quad (26)$$

$$\begin{aligned} \tilde{f}_\tau &= f(\tilde{y}_+, \tilde{y}_-, y) = \frac{y^2}{2} [2 + y^2 + \tau |1 + y| (2 - y)], \\ \tau &= \text{sign}(y_+ y - y), \quad \tilde{f}_\pm \equiv \tilde{f}_{\pm 1}, \end{aligned} \quad (27)$$

$$\begin{aligned} \hat{\mathcal{I}}_\pm &\simeq \int_0^\infty \frac{dy_+}{(y_+^2 - (\tilde{y}_+ - i0)^2)} \int_0^\infty \frac{dy_-}{(y_-^2 - (\tilde{y}_- - i0)^2)} \\ &\times \frac{T^D(z_v y - s) + T^D(-z_v y - s)}{z_v^2 y_-^2} \theta(y \pm 4y_+ y_-), \end{aligned} \quad (28)$$

where $1/z_v$ is replaced by infinities in the upper limits, and z_m is set to zero in the denominator ($y_-^2 + z_m^2 y$). These replacements do not change much the final result, but significantly simplify further calculations. Contribution of residues in (28) is dominant, if we take into account only the imaginary part of the amplitude T^D (which is rather good approximation in most interesting cases), and we can write in this case

$$\mathcal{I}_V \simeq -\frac{\pi^2}{2} \int_0^1 \frac{dy}{y(1+y)} (y+4) T^D\left(\frac{y s}{2}\right). \quad (29)$$

As to the denominator, there are simple arguments to set z_m to zero. Since $T^D(0) = 0$, and the contribution from

the region $s y/2 > m^2$ (i.e. $y > 2z_m^2$) is dominant, we have

$$\begin{aligned} y_-^2 + y z_m^2 &\simeq y \left(\frac{y}{4z_v^2} + z_m^2 \right), \\ \frac{y}{4z_v^2} &> \frac{z_m^2}{2z_v^2} \gg z_m^2. \end{aligned} \quad (30)$$

Now we can extract parameters for the amplitude T^D of the process $g + p \rightarrow g + p$. If we use the model of vector dominance, the amplitude of the photoproduction looks as

$$\mathcal{M}_{i,i}^{\gamma+p \rightarrow V+p} = \frac{3\pi^2}{8\alpha_s(m_V^2)} \bar{\mathcal{K}}_V \mathcal{M}_{i,i}^{V^*+p \rightarrow V+p}. \quad (31)$$

We can fix parameters of a model for meson-proton scattering by fitting the data on photoproduction. Then we can use expression (22) and compare it with (31). Finally we can obtain the amplitude of gluon-proton scattering from the equality

$$\mathcal{I}_V = \frac{3\pi^2}{8\alpha_s(m_V^2)} \mathcal{M}_{i,i}^{V^*+p \rightarrow V+p}. \quad (32)$$

In the above expressions we do not take into account the dependence of \mathcal{I}_V on t , since it is rather weak. It comes from the diffractive amplitude $T^D \equiv T^D(s, t)$. It means that (22), (23), (28), (29) and (32) are taken at any fixed value of t . If we use the data on total cross-sections we have to use the following equality:

$$\begin{aligned} &\int_{t_{\min}}^{t_{\max}} dt |\mathcal{I}_V(s, t)|^2 \\ &= \left(\frac{3\pi^2}{8\alpha_s(m_V^2)} \right)^2 \int_{t_{\min}}^{t_{\max}} dt \left| \mathcal{M}_{i,i}^{V^*+p \rightarrow V+p}(s, t) \right|^2. \end{aligned} \quad (33)$$

2.3 3-Pomeron model as an example for calculations.

Let us stress that in this paper calculations of integrals do not depend on the form of gluon-proton scattering amplitude T^D . In principle, we can use any model it. For example, in the case of the ordinary unintegrated gluon distribution

$$T^D\left(\frac{y s}{2}\right) \simeq T^D\left(\frac{\kappa^2}{x}\right) \implies f_g(x, \kappa^2, \mu^2), \quad x = \frac{m_V^2}{s}, \quad (34)$$

and the integral (29) can be rewritten as

$$\mathcal{I}_V \sim -2\pi^2 \int_{\kappa_0^2}^{s/2} \frac{d\kappa^2}{\kappa^2} f_g(x, \kappa^2, \mu^2), \quad (35)$$

which can be finally expressed in terms of the integrated parton distribution $f_g(x, \mu^2)$.

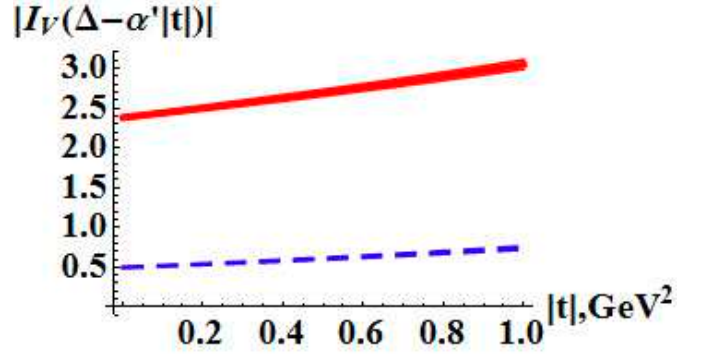


Fig. 3. Function $|I_V(\Delta - \alpha'|t)|$ versus $|t|$ for $m_V = m_{J/\psi} = 3.1$ GeV (solid) and $m_V = m_\Upsilon = 9.46$ GeV (dashed).

2.3.1 Extraction of the model parameter in the 3-Pomeron model

As a quantitative example, in this section we consider the case of the modified Regge-eikonal model with three Pomerons [47]. Model parameters with errors and fits to the data on J/Ψ photoproduction can be found in [46]. It is clear from [46] that the main contribution to the amplitude comes from the “Born term” of the so called “hard” (“3rd”) Pomeron in the model. Let us write corresponding amplitudes and use (32) to extract the coupling for the gluon-proton amplitude T^D :

$$T^D \simeq \eta_{P_3} c_{gp}^{(3)} e^{B_0^{(3)} t} \left(\frac{2p\kappa}{s_0 - \kappa^2} \right)^{\alpha_{P_3}(t)}, \quad (36)$$

$$\mathcal{I}_V = I_V c_{gp}^{(3)} \eta_{P_3} e^{B_0^{(3)} t} \left(\frac{s}{s_0} \right)^{\alpha_{P_3}(t)}, \quad (37)$$

$$\mathcal{M}_{i,i}^{V^*+p \rightarrow V+p} = c_{Vp}^{(3)} \eta_{P_3} e^{B_0^{(3)} t} \left(\frac{s}{s_0} \right)^{\alpha_{P_3}(t)} \quad (38)$$

$$B_0^{(3)} = \frac{1}{4} (r_{pP_3}^2 + r_{gP_3}^2), \quad (39)$$

$$\alpha_{P_3}(t) = 1 + \Delta + \alpha' t, \quad \Delta = 0.2032 \pm 0.0041, \quad \alpha' = 0.0937 \pm 0.0029 \text{ GeV}^{-2}, \quad (40)$$

$$r_{pP_3}^2 = (2.4771 \pm 0.0964) \text{ GeV}^{-2}, \quad r_{gP_3}^2 = (2.54 \pm 0.41) \text{ GeV}^{-2}, \quad (41)$$

$$c_{J/\Psi p}^{(3)} = 1.11 \pm 0.07, \quad \chi^2/dof = 1.48. \quad (42)$$

From (32) we have

$$c_{gp}^{(3)} = \frac{3\pi^2}{8\alpha_s(m_V^2)} |I_V| c_{Vp}^{(3)}. \quad (43)$$

With rather good accuracy of about 1% it is possible to calculate $|I_V|$:

$$|I_V| \simeq \frac{\pi^2}{2^{2+\Delta}} \int_0^1 \frac{dy y^\Delta (4+y)}{(1+y)(1+y/y_0)^{\Delta+1}}, \quad (44)$$

where $\Delta = \alpha_{P_3}(t) - 1$. $|I_V|$ as a function of $|t|$ is depicted in the Fig. 3.

Since in [46] the fitting procedure was done for the data in the interval $0 < |t| < 1 \text{ GeV}^2$ we have to use more general equation (33), which leads to the replacement

$$|I_V| \implies \langle I_V \rangle = \sqrt{\frac{\int_0^1 d|t| e^{-2B|t|} |I_V|^2}{\int_0^1 d|t| e^{-2B|t|}}} \quad (45)$$

in (43), where $B = B_0^{(3)} + \alpha' \ln(s/s_0)$. Finally we get the coupling value

$$c_{gp}^{(3)} = 6.535 \pm 0.418. \quad (46)$$

Here we use another definitions and prescriptions for calculations in comparison with [46], that is why the value of c_{gp} is different. It is more correct than in [46] and further we will use the definitions and formulae of the present paper for convenience. Errors of c_{gp} are estimated from the errors of all the parameters in (43) with the replacement (45).

2.3.2 Predictions for J/Ψ to Υ production ratio.

Coupling constant $c_{gp}^{(3)}$ have to be the same for any produced vector meson. We can use this fact to check the model predictions for J/Ψ and Υ mesons. For the total cross-sections ratio it is possible to write

$$\begin{aligned} \mathcal{R}_{th.} &= \frac{\sigma_{\gamma p \rightarrow \Upsilon p}(W_\Upsilon)}{\sigma_{\gamma p \rightarrow J/\Psi p}(W_{J/\Psi})} \\ &\simeq \left(\frac{\alpha_s(m_\Upsilon)^2 \langle I_\Upsilon \rangle (m_\Upsilon, W_\Upsilon) W_\Upsilon^\Delta}{\alpha_s(m_{J/\Psi}^2) \langle I_{J/\Psi} \rangle (m_{J/\Psi}, W_{J/\Psi}) W_{J/\Psi}^\Delta} \right)^2 \\ &\times \frac{\Gamma_{\Upsilon \rightarrow e^+e^-}}{m_\Upsilon} \frac{\Gamma_{J/\Psi \rightarrow e^+e^-}}{m_{J/\Psi}}, \end{aligned} \quad (47)$$

where

$$\begin{aligned} m_{J/\Psi} &= 3.1 \text{ GeV}, \quad \alpha_s(m_{J/\Psi}^2) = 0.25, \\ \Gamma_{J/\Psi \rightarrow e^+e^-} &= 5.52 \pm 0.18 \text{ keV}, \end{aligned} \quad (48)$$

$$\begin{aligned} m_\Upsilon &= 9.46 \text{ GeV}, \quad \alpha_s(m_\Upsilon^2) = 0.182, \\ \Gamma_{\Upsilon \rightarrow e^+e^-} &= 1.34 \pm 0.05 \text{ keV}. \end{aligned} \quad (49)$$

Results of comparison based on the experimental data [69]-[71] are presented in the Table 1. As you can see the model adequately describes the data.

3 Exclusive double diffractive events.

In this section we consider the exclusive central diffraction. The previous simple model with three Pomerons was presented in [14]-[16]. Here is the more general approach.

Table 1. Theoretical predictions and experimental results for the ratio \mathcal{R} at different values of collision energies of J/Ψ and Υ photoproduction. Experimental data are taken from [69]-[71].

$W_{J/\Psi}$, GeV	W_Υ , GeV	$\mathcal{R}_{exp.} \times 10^3$	$\mathcal{R}_{th.} \times 10^3$
20-30	60-130	4.91 ± 2.23	3.49 ± 0.64
20-30	130-220	9.85 ± 4.37	4.43 ± 0.66
20-30	60-220	7.21 ± 2.45	4.06 ± 1.03
30-50	60-130	3.86 ± 1.55	2.89 ± 0.56
30-50	130-220	7.73 ± 3.0	3.68 ± 0.59
30-50	60-220	5.66 ± 1.49	3.37 ± 0.88
50-70	60-130	2.87 ± 1.15	2.47 ± 0.44
50-70	130-220	5.75 ± 2.24	3.13 ± 0.44
50-70	60-220	4.21 ± 1.12	2.87 ± 0.72
70-90	60-130	2.4 ± 0.99	2.2 ± 0.38
70-90	130-220	4.82 ± 1.9	2.79 ± 0.37
70-90	60-220	3.53 ± 0.96	2.56 ± 0.63
90-110	60-130	2.18 ± 0.88	2.01 ± 0.34
90-110	130-220	4.37 ± 1.7	2.56 ± 0.33
90-110	60-220	3.2 ± 0.85	2.34 ± 0.57
110-130	60-130	1.85 ± 0.74	1.87 ± 0.31
110-130	130-220	3.7 ± 1.44	2.38 ± 0.3
110-130	60-220	2.71 ± 0.71	2.18 ± 0.53
130-150	60-130	1.54 ± 0.63	1.76 ± 0.29
130-150	130-220	3.09 ± 1.23	2.24 ± 0.28
130-150	60-220	2.26 ± 0.63	2.05 ± 0.5
150-170	60-130	1.46 ± 0.61	1.67 ± 0.28
150-170	130-220	2.92 ± 1.19	2.12 ± 0.27
150-170	60-220	2.14 ± 0.62	1.94 ± 0.47

3.1 Kinematics.

Let us remind to the reader some kinematical formulae. In the Fig. 4 we illustrate the perturbative mechanism for the “bare” amplitude of the process $p+p \rightarrow p+M+p$. We use the kinematics, which corresponds to the double Regge limit. It is convenient to use light-cone representation for momenta. The notations are

$$\begin{aligned} s &= (p_1 + p_2)^2, \quad s' = (p'_1 + p'_2)^2, \\ \bar{s} &= p_1 p_2 + \sqrt{(p_1 p_2)^2 - m^4} = \frac{s - 2m^2}{2} + \frac{s}{2} \sqrt{1 - \frac{4m^2}{s}}, \\ p_1 &= \left\{ \sqrt{\frac{\bar{s}}{2}}, \frac{m^2}{\sqrt{2\bar{s}}}; \mathbf{0} \right\}, \quad p_2 = \left\{ \frac{m^2}{\sqrt{2\bar{s}}}, \sqrt{\frac{\bar{s}}{2}}; \mathbf{0} \right\}, \\ p'_1 &= p_1 - \Delta_1 = \left\{ (1 - \xi_1) \sqrt{\frac{\bar{s}}{2}}, \frac{\Delta_1^2 + m^2}{(1 - \xi_1) \sqrt{2\bar{s}}}; -\Delta_1 \right\}, \\ p'_2 &= p_2 - \Delta_2 = \left\{ \frac{\Delta_2^2 + m^2}{(1 - \xi_2) \sqrt{2\bar{s}}}, (1 - \xi_2) \sqrt{\frac{\bar{s}}{2}}; -\Delta_2 \right\}, \\ \tilde{p}_1 &= p_1 - \frac{m^2}{\bar{s}} p_2 = \left\{ \sqrt{\frac{\bar{s}}{2}} \left(1 - \frac{m^4}{\bar{s}^2} \right), 0; \mathbf{0} \right\}, \\ \tilde{p}_2 &= p_2 - \frac{m^2}{\bar{s}} p_1 = \left\{ 0, \sqrt{\frac{\bar{s}}{2}} \left(1 - \frac{m^4}{\bar{s}^2} \right); \mathbf{0} \right\}, \\ p_{1,2}^2 &= p'_{1,2}{}^2 = m^2, \quad \tilde{p}_{1,2}^2 = 0, \end{aligned} \quad (50)$$

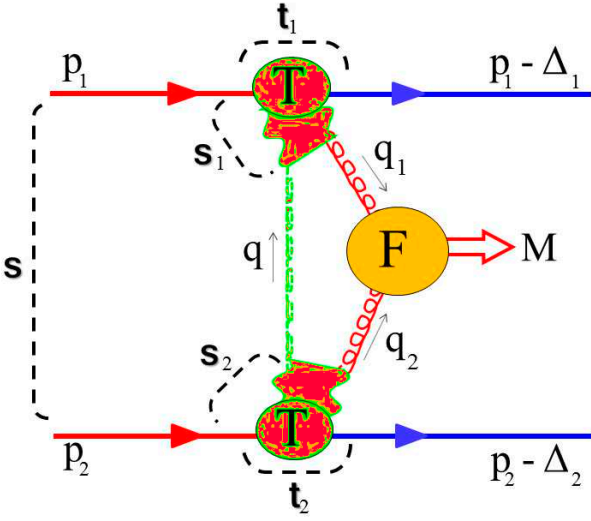


Fig. 4. “Bare” amplitude and kinematics of the Exclusive Double Diffractive Event (EDDE) in the case of perturbative Pomeron-Pomeron fusion. Absorption in the initial and final pp channels is not shown.

$$q = \sqrt{\frac{2}{s}}(q_+ \tilde{p}_1 + q_- \tilde{p}_2) + q_\perp = \{q_+, q_-, \mathbf{q}\},$$

$$q_1 = q + \Delta_1, \quad q_2 = -q + \Delta_2, \quad \Delta_{1,2} \simeq \xi_{1,2} \tilde{p}_{1,2}, \quad (51)$$

where $\xi_{1,2}$ are fractions of protons’ momenta carried by gluons. From the above notations we can obtain the relations:

$$t_{1,2} = \Delta_{1,2}^2 \simeq -\frac{\Delta_{1,2}^2 + \xi_{1,2}^2 m^2}{1 - \xi_{1,2}} \simeq -\Delta_{1,2}^2, \quad \xi_{1,2} \rightarrow 0$$

$$M^2 = (q_1 + q_2)^2 \simeq \xi_1 \xi_2 s + t_1 + t_2 - 2\sqrt{t_1 t_2} \cos \phi_0$$

$$M_\perp^2 = \xi_1 \xi_2 s \simeq M^2 + |t_1| + |t_2| + 2\sqrt{t_1 t_2} \cos \phi_0$$

$$\cos \phi_0 = \frac{\Delta_1 \Delta_2}{|\Delta_1| |\Delta_2|} \quad (52)$$

$$s_1 = (p_1 + q)^2 \simeq m^2 + q^2 + \sqrt{2s} q_-$$

$$s_2 = (p_2 - q)^2 \simeq m^2 + q^2 - \sqrt{2s} q_+ . \quad (53)$$

Physical region of diffractive events with two rapidity gaps is defined by the following kinematical cuts:

$$0.01 \text{ GeV}^2 \leq |t_{1,2}| \leq \sim 1 \text{ GeV}^2, \quad (54)$$

$$\xi_{min} \simeq \frac{M^2}{s \xi_{max}} \leq \xi_{1,2} \leq \xi_{max} \sim 0.1, \quad (55)$$

$$(\sqrt{-t_1} - \sqrt{-t_2})^2 \leq \kappa \leq (\sqrt{-t_1} + \sqrt{-t_2})^2 \quad (56)$$

$$\kappa = \xi_1 \xi_2 s - M^2 \ll M^2$$

We can write the relations in terms of $y_{1,2}$ and y (rapidities of hadrons and the system M correspondingly). For instance:

$$\xi_{1,2} \simeq \frac{M}{\sqrt{s}} e^{\pm y}, \quad |y| \leq y_0 = \ln \left(\frac{\sqrt{s} \xi_{max}}{M} \right),$$

$$|y_{1,2}| = \frac{1}{2} \ln \frac{(1 - \xi_{1,2})^2 s}{m^2 - t_{1,2}} \geq 9. \quad (57)$$

3.2 Basic ingredients.

Let us consider basic constituents of the model framework. We begin from the case of perturbative representation of the Pomeron-Pomeron fusion as depicted in Fig. 4 and in Fig. 5a. In the perturbative case we have to use proton-gluon amplitudes T convoluted with gluon-gluon fusion amplitude F (see Fig. 4), then take into account Sudakov-like suppression (depicted by curved wavy lines in Fig. 5a), and, finally, absorptive (or rescattering) corrections denoted by V -blobs. In the nonperturbative case it is not possible to consider Pomeron as a singlet two-gluon state, and we also have to take into account the interaction between the central low mass state with the protons (blobs with the dashed boundary in the Fig. 5c). Recently it was shown in [13] that enhanced diagrams (additional soft interactions) can play significant role.

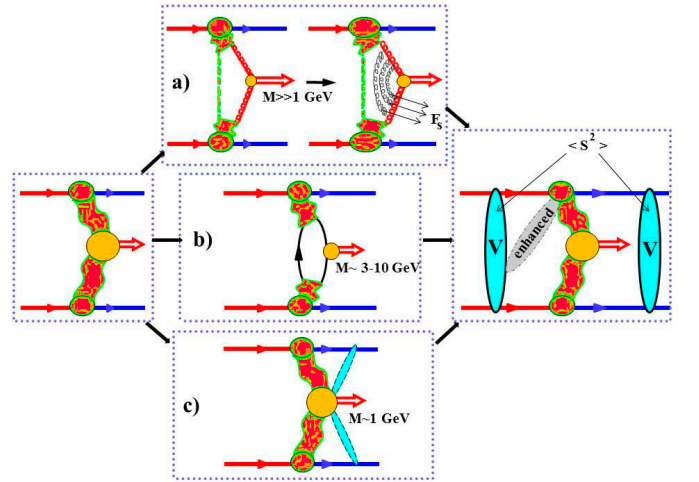


Fig. 5. Scheme of calculation of the full EDDE amplitude in the case of high (a), intermediate (b) and low (c) invariant mass, i.e. perturbative, intermediate and nonperturbative Pomeron-Pomeron fusion correspondingly.

3.2.1 Proton-gluon scattering.

Diffractive part T of the amplitude is calculated the same way as in (14):

$$T_1^{\alpha\mu} \equiv T^{\alpha\mu}(p_1, -q, q_1), \quad T_2^{\alpha\nu} \equiv T^{\alpha\nu}(p_2, q, q_2) \quad (58)$$

Here we take apart color delta-functions in all amplitudes, which give overall factor 8 after contractions and neglect terms of the order $o(\xi_i)$, $o(t_i/m^2)$. Equations (16) are used to simplify calculations.

3.2.2 Gluon-gluon fusion.

The main contribution to the gluon-gluon fusion tensor can be represented as

$$F_{\mu\nu} = G_{\mu\nu} F_{gg \rightarrow M}, \quad G_{\mu\nu} = g_{\mu\nu} - \frac{q_{2,\mu} q_{1,\nu}}{q_1 q_2}, \quad (59)$$

where $F_{gg \rightarrow M}$ is related to the differential cross-section

$$\frac{d\hat{\sigma}_{gg \rightarrow M}}{d\hat{t}} = \frac{1}{(2s_g^{(1)} + 1)(2s_g^{(2)} + 1)N_g^2} N_g \times |F_{gg \rightarrow M}|^2 \frac{\sum_{i=1}^2 |G_{\mu\nu} \epsilon_i^\mu \epsilon_i^\nu|^2}{16\pi M^4}, \quad (60)$$

where

$$N_g = N_c^2 - 1 = 8, \quad 2s_g^{(i)} + 1 = 2 \quad (q_i^2 = 0),$$

$$|F_{gg \rightarrow M}|^2 = 256\pi M^4 \frac{d\hat{\sigma}_{gg \rightarrow M}}{d\hat{t}},$$

and $M = gg, Q\bar{Q}, \gamma\gamma, W^+W^-, ZZ$ or other two-particle system with final momenta $k_{1,2}$ and $\hat{t} = (q_1 - k_1)^2$. For one particle production ($M = H, G(\text{graviton}), \chi_{b,c}$) $F_{gg \rightarrow M}$ can be expressed in terms of the hadronic decay width of a particle

$$|F_{gg \rightarrow M}|^2 = 64\pi^2 \frac{\Gamma_{M \rightarrow gg}}{M}. \quad (61)$$

Here we neglect other transverse tensor structure in $F_{\mu\nu}$ proportional to $q_1, \mu q_2, \nu$ since it gives small contribution to the result.

3.2.3 Sudakov-like suppression.

In the perturbative case there is an additional factor for the gluon-gluon fusion vertex, which is depicted as virtual gluon corrections in Fig. 5a. If we take into account the emission of virtual "soft" gluons, while prohibiting the real ones, that could fill rapidity gaps, this results in the Sudakov-like suppression [80]:

$$F_s(l^2, \mu^2) = \exp \left[- \int_{l^2}^{\mu^2} \frac{dp_T^2}{p_T^2} \frac{\alpha_s(p_T^2)}{2\pi} \int_{\Delta(\mu)}^{1-\Delta(\mu)} z P_{gg}(z) dz + \int_0^1 \sum_q P_{qg}(z) dz \right]. \quad (62)$$

Here

$$P_{gg}(z) = 6 \frac{(1-z(1-z))^2}{z(1-z)},$$

$$\Delta(\mu) = \frac{p_T}{p_T + \mu}, \quad l^2 = -q^2, \quad \mu = M/2, \quad (63)$$

and q is the loop momentum in Fig. 4.

3.2.4 Soft rescattering.

We have to take into account also the hadron-hadron "soft" interaction in the initial and in the final states (unitary

corrections or re-scattering). It is denoted by V in Fig. 5 and given by the following analytical expressions:

$$\mathcal{M}^U(p_1, p_2, \Delta_1, \Delta_2) = \int \frac{d^2 \mathbf{q}_T}{(2\pi)^2} \frac{d^2 \mathbf{q}'_T}{(2\pi)^2} V(s, \mathbf{q}_T) \times \mathcal{M}(p_1 - q_T, p_2 + q_T, \Delta_{1T}, \Delta_{2T}) V(s', \mathbf{q}'_T), \quad (64)$$

$$V(s, \mathbf{q}_T) = \int d^2 \mathbf{b} e^{i\mathbf{q}_T \mathbf{b}} \sqrt{1 + 2i T_{pp \rightarrow pp}^{el}(s, \mathbf{b})}, \quad (65)$$

where $\Delta_{1T} = \Delta_1 - q_T - q'_T$, $\Delta_{2T} = \Delta_2 + q_T + q'_T$, \mathcal{M} is the "bare" amplitude of the process $p + p \rightarrow p + M + p$. In the case of the eikonal representation of the elastic amplitude $T_{pp \rightarrow pp}^{el}$ we have

$$V(s, \mathbf{q}_T) = \int d^2 \mathbf{b} e^{i\mathbf{q}_T \mathbf{b}} e^{i\delta_{pp \rightarrow pp}(s, \mathbf{b})}, \quad (66)$$

where $\delta_{pp \rightarrow pp}$ is the eikonal function. As was shown in [59], these "outer" unitary corrections strongly reduce the value of the corresponding cross-section and change the azimuthal angle dependence. The ratio

$$\langle S^2 \rangle = \frac{\int \int d^2 \mathbf{\Delta}_1 d^2 \mathbf{\Delta}_2 |\mathcal{M}^U|^2}{\int \int d^2 \mathbf{\Delta}_1 d^2 \mathbf{\Delta}_2 |\mathcal{M}|^2} \quad (67)$$

is usually called "soft survival probability".

3.2.5 Full construction. Convolution and integration. EDDE luminosity.

Let us collect all the ingredients of the framework. First of all we calculate the loop integral

$$\mathcal{I}_q = 2\pi \int \frac{d^4 q}{(2\pi)^4} \frac{f(q_+, q_-, \mathbf{q}^2, \dots)}{(q^2 + i0)(q_1^2 + i0)(q_2^2 + i0)},$$

$$q_1^2 + i0 \simeq \pm \sqrt{2s} \xi_1 \left(q_{\mp} \pm \left(\frac{\mathbf{q}_1^2}{\sqrt{2s} \xi_1} - i0 \right) \right), \quad (68)$$

factor 2π before the integral is introduced for convenience. It was shown in [81], that the leading contribution arises from the region of the integration, where momentum q is "Glauber-like", i.e. of the order $(k_+ m^2 / \sqrt{s}, k_- m^2 / \sqrt{s}, \mathbf{k}m)$, where k 's are of the order 1. The detailed consideration of the loop integral shows that the main contribution comes from the poles at $q_i^2 = 0$

$$\mathcal{I}_q = \frac{1}{2^4 M^2} \int_0^{\frac{M^2}{4}} \frac{d\mathbf{q}^2 f(-\frac{\mathbf{q}_2^2}{\sqrt{2s}\xi_2}, \frac{\mathbf{q}_1^2}{\sqrt{2s}\xi_1}, \mathbf{q}^2, \dots)}{\left(\mathbf{q}^2 + \frac{\mathbf{q}_1^2 \mathbf{q}_2^2}{M^2} \right)},$$

$$\mathbf{q}_2^2 = \mathbf{q}^2 + \Delta_1^2 \pm 2|\mathbf{q}| |\Delta_1| \cos(\phi \pm \frac{\phi_0}{2}). \quad (69)$$

As to the lower limit in the integral (69), we set it to zero since $f|_{\mathbf{q}^2=0} = 0$ and the main contribution comes from the region $\mathbf{q}_i^2 / \xi_i > m^2$, which gives $\mathbf{q}^2 > \langle |t_i| \rangle \sim 0$.

In our case we have to replace the function f in (69) by

$$\begin{aligned}\tilde{f} &= 8F_{\mu\nu}T_1^{\alpha\mu}T_2^{\alpha\nu}F_s(-q^2, \frac{M^2}{4}) \\ &\simeq 8\frac{2M^2\mathbf{q}_1\mathbf{q}_2}{\mathbf{q}_1^2\mathbf{q}_2^2}F_s(q^2, \frac{M^2}{4})T_1^DT_2^DF_{gg\rightarrow M}, \\ T_{\frac{1}{2}}^D &\equiv T^D\left(\frac{\sqrt{s}}{M}e^{\mp y}\mathbf{q}_{\frac{1}{2}}^2\sqrt{1-\frac{M}{\sqrt{s}}e^{\pm y}}\right)\end{aligned}\quad (70)$$

Finally to obtain the EDDE cross-section we can introduce the luminosity function

$$\hat{\mathcal{L}}_{EDDE} = \frac{1}{2^9\pi^6}\left(\frac{M^2}{s}\right)^2|\mathcal{I}_q|^2\langle S^2\rangle, \quad (71)$$

where for low values of $\Delta_{1,2}$ we replace $\mathbf{q}_{1,2}$ by \mathbf{q} in \mathcal{I}_q . Now we can write

$$M^2\frac{d\sigma_{EDDE}}{dM^2 dy d\Phi_{gg\rightarrow M}} = \hat{\mathcal{L}}_{EDDE}\frac{d\hat{\sigma}_{gg\rightarrow M}^{J_z=0}}{d\Phi_{gg\rightarrow M}}. \quad (72)$$

For resonance production Eq. (72) can be simplified to

$$\frac{d\sigma_{EDDE}^{Res}}{dy} = \hat{\mathcal{L}}_{EDDE}\frac{2\pi^2\Gamma_{M\rightarrow gg}}{M^3}, \quad (73)$$

where $\Gamma_{M\rightarrow gg}$ is the resonance width.

As in the case of EVMP we can use any model for T^D . For example,

$$T^D\left(\frac{\mathbf{q}^2}{\xi}\sqrt{1-\xi}\right) \implies f_g(\xi, \mathbf{q}^2, \mu^2). \quad (74)$$

Gluon-gluon fusion functions can be found in the Appendix A.

3.2.6 3-Pomeron model as an example.

In the 3-Pomeron model the diffractive proton-gluon amplitude is similar to (36)

$$T_i^D \simeq \eta_{P_3}c_{gp}^{(3)}e^{B_0^{(3)}t_i}\left(\frac{s_i - m^2 - qq_i}{s_0 - qq_i}\right)^{\alpha_{P_3}(t_i)}, \quad (75)$$

and for the EDDE luminosity we have

$$\begin{aligned}\hat{\mathcal{L}}_{EDDE} &= \frac{|\eta_{P_3}c_{gp}^{(3)}|^4}{2^9\pi^6}\frac{1}{4B^2}\left(\frac{s}{M^2}\right)^{2\Delta} \\ &\times\left(1 - \frac{2M}{\sqrt{s}}\cosh y + \frac{M^2}{s}\right)^\Delta|\mathcal{I}_q|^2\langle S^2\rangle,\end{aligned}\quad (76)$$

where

$$\begin{aligned}\mathcal{I}_q &= \int_{\langle|t_i|\rangle}^{\frac{M^2}{4}}\frac{d\mathbf{q}^2}{\mathbf{q}^2}(\mathbf{q}_1\mathbf{q}_2) \\ &\times\frac{(\mathbf{q}_1^2)^{\alpha_{P_3}(t_1)-1}(\mathbf{q}_2^2)^{\alpha_{P_3}(t_2)-1}}{(s_0 + \mathbf{q}^2/2)^{\alpha_{P_3}(t_1)+\alpha_{P_3}(t_2)}}F_s\left(\mathbf{q}^2, \frac{M^2}{4}\right) \\ &\simeq -\int_0^{\frac{M^2}{4}}d\mathbf{q}^2\frac{(\mathbf{q}^2)^{2\Delta}}{(s_0 + \mathbf{q}^2/2)^{2(1+\Delta)}}F_s\left(\mathbf{q}^2, \frac{M^2}{4}\right),\end{aligned}\quad (77)$$

and the ‘‘soft survival probability’’ can be reduced to the simple form (see Appendix B):

$$\langle S^2\rangle \simeq \frac{1}{4B}\int_0^\infty|h(\tau)|^2d\tau^2, \quad (78)$$

$$h(\tau) = \int_0^\infty b db J_0(b\tau)e^{-\Omega(s,b)-\Omega(s',b)-b^2/(8B)}, \quad (79)$$

where $B = B_0^{(3)} + \alpha'\ln(\sqrt{s}/M)$, $\Omega \equiv i\delta_{pp\rightarrow pp}$, and $\delta_{pp\rightarrow pp}$ can be found in [47]. Functions $\langle S^2\rangle$, $|\mathcal{I}_q|^2$ and $\hat{\mathcal{L}}_{EDDE}$ are presented in Figs 6, 7, 8.

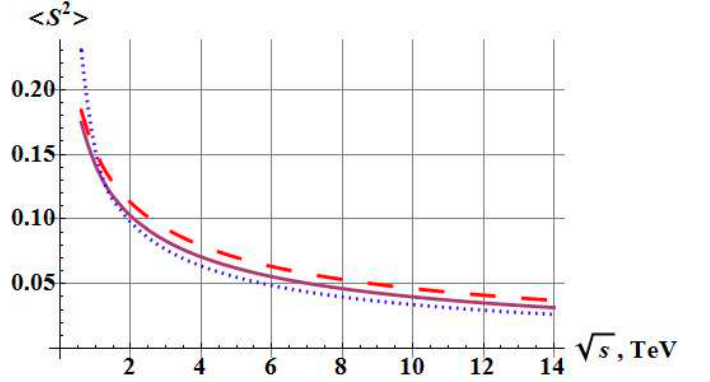


Fig. 6. ‘‘Soft survival probability’’ in the case of the 3-Pomeron model for different values of the invariant mass: $M = 30$ GeV (dashed), $M = 125$ GeV (solid) and $M = 600$ GeV (dotted).

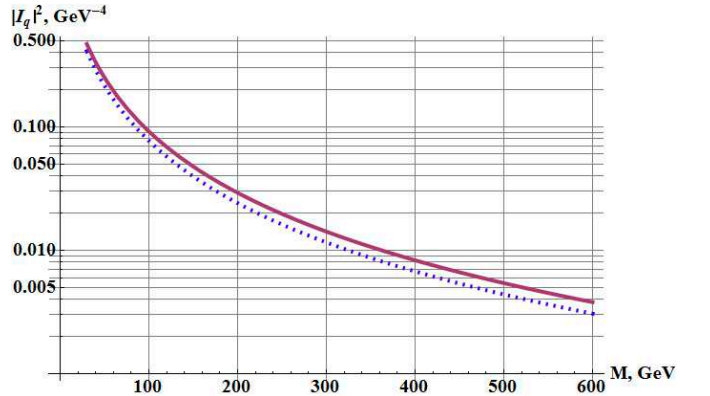


Fig. 7. Function $|\mathcal{I}_q|^2$ versus M for different values of the parameter Δ in the case of the 3-Pomeron model. $\Delta = \alpha_{P_3}(0) - 1$ (solid) and $\Delta = \alpha_{P_3}(1) - 1$ (dotted).

3.2.7 Nonperturbative mechanism of Pomeron-Pomeron fusion. Discussion.

If the central mass produced in EDDE is low (about several GeV), it is not possible to use perturbative repre-

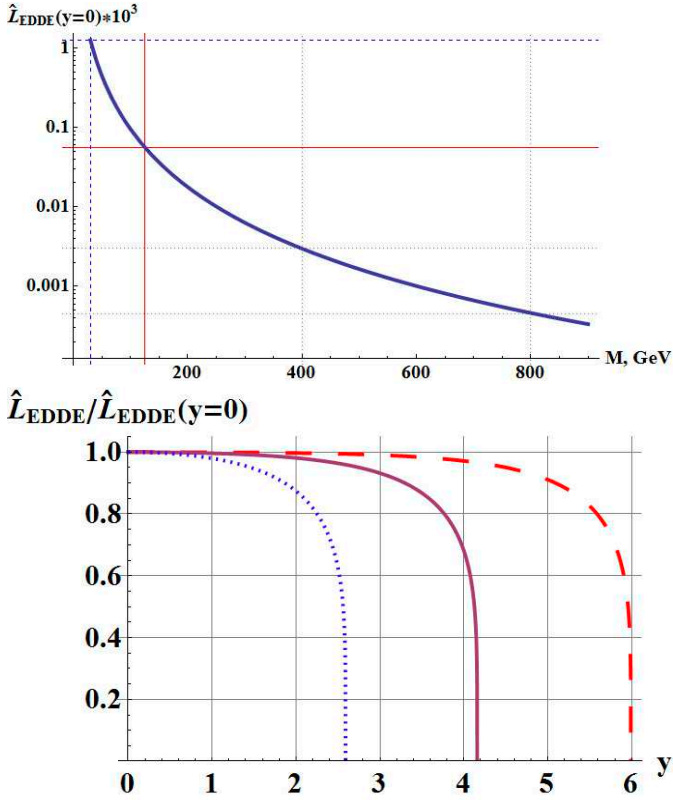


Fig. 8. Pomeron-Pomeron luminosity $\hat{\mathcal{L}}_{EDDE}$ at $y = 0$ (top picture) and as a function of y for different fixed invariant masses (bottom picture) in the case of the 3-Pomeron model. In the left picture solid grid line denotes $M = 125$ GeV and dashed one denotes $M = 30$ GeV. In the right picture curves correspond to $M = 20$ GeV (dashed), $M = 125$ GeV (solid) and $M = 600$ GeV (dotted).

sensation (see Fig. 4 and Fig. 5a) for the amplitude of the process, and we have to use more general “nonperturbative” form (see Fig. 5c). In this case we have to obtain somehow the vertex “Pomeron-Pomeron-Central system”.

From the first principles we can write the general structure of the vertex for different cases [59]. For example, for the production of the system with J^P (spin-parity) we have

$$|\mathcal{M}^{0+}|^2 \sim (M_{\perp}^2)^{2(\alpha_{\mathbb{P}}(0)-1)} (f_0 M_{\perp}^2 + 2f_1)^2, \quad (80)$$

$$|\mathcal{M}^{0-}|^2 \sim (M_{\perp}^2)^{2(\alpha_{\mathbb{P}}(0)-1)} f_0 t_1 t_2 \sin^2 \phi_0, \quad (81)$$

$$|\mathcal{M}^{1+}|^2 \sim (M_{\perp}^2)^{2(\alpha_{\mathbb{P}}(0)-1)} (\mathcal{F}_0 M_{\perp}^4 + \mathcal{F}_1 t_1 t_2 \sin^2 \phi_0 + \mathcal{F}_2), \quad (82)$$

$$\mathcal{F}_{0,2} \sim o(t_i),$$

$$|\mathcal{M}^{2+}|^2 \sim (M_{\perp}^2)^{2(\alpha_{\mathbb{P}}(0)-1)} (\mathcal{F}_0 M_{\perp}^4 + \mathcal{F}_1 M_{\perp}^2 + \mathcal{F}_2), \quad (83)$$

with notations (52),(53) and functions defined in [59]. The general structure of helicity amplitudes from the simple Regge behaviour was also considered in [55],[56]. Experimental data are in good agreement with these predictions.

There are some attempts to obtain the vertex in special models for the Pomeron. In Refs. [57],[58] results were

obtained from the assumption that the Pomeron acts as a 1^+ conserved or nonconserved current. The Pomeron-Pomeron fusion based on the “instanton” or “glueball” dynamics was considered in [19]-[22]. You can see also recent papers [23],[24] devoted to calculations of the Pomeron-Pomeron fusion vertex in the nonperturbative regime.

3.3 Standard candles for high invariant masses.

One of the basic tasks now is to make predictions for EDDE with production of fundamental particles like the Higgs boson. First of all we can check any theoretical model by the use of the recent data from Tevatron [38]-[44]. “Standard candles” in the case of high invariant mass are exclusive central di-jet and di-gamma production. We can use also $\chi_{c,0}$ production, but $m_{\chi_{c,0}} = 3.5$ GeV and we have to take into account also nonperturbative mechanisms of the Pomeron-Pomeron fusion.

Let us analyse the CDF data in the framework of the 3-Pomeron model. In Fig. 9 you can see the prediction based on the HERA data (upper dotted curve) with the value of $c_{gp}^{(3)}$ presented in (46). As was claimed in [11],[12], the uncertainty on the hadronic level can be taken into account by rescaling of jet E_T . After application of this procedure to our result with $E_{T,jet} = 0.75E_{T,g}$ we obtain the lower dashed curve in Fig. 9, which is in quite a good agreement with the CDF data.

The prediction for the exclusive central di-gamma production is shown in Fig. 10. The value of the predicted cross-section after CDF cuts are

$$E_T > 5 \text{ GeV}, |\eta_{\gamma}| < 1 \implies \sigma_{\gamma\gamma}^{excl, th} = 28 \pm 8 \text{ fb}, \quad (84)$$

$$E_T > 2.5 \text{ GeV}, |\eta_{\gamma}| < 1 \implies \sigma_{\gamma\gamma}^{excl, th} = 0.29 \pm 0.08 \text{ pb}, \quad (85)$$

which are close to the predictions [13]. As was shown in [13], uncertainties in the gluon distributions can lead

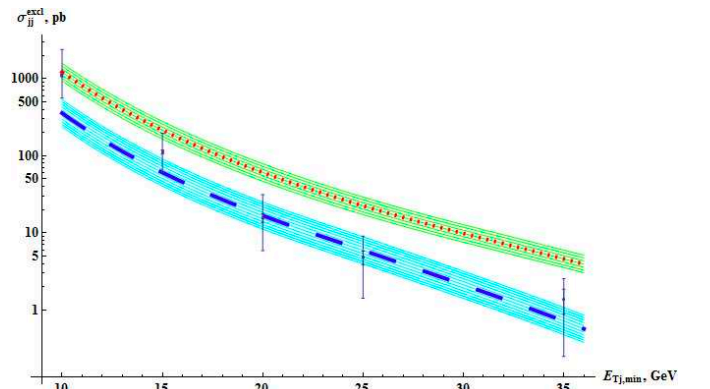


Fig. 9. CDF data on the exclusive di-jet production cross-section [39] versus the lower cut of $E_{T,jet}$ and the prediction of the 3P-model. Upper dotted curve corresponds to the value of $c_{gp}^{(3)}$ presented in (46) and obtained from fitting the HERA data on EVMP. Lower dashed curve is obtained by rescaling $E_{T,jet} = 0.75E_{T,g}$ as was proposed in [11],[12]. Filled areas denote errors from $c_{gp}^{(3)}$.

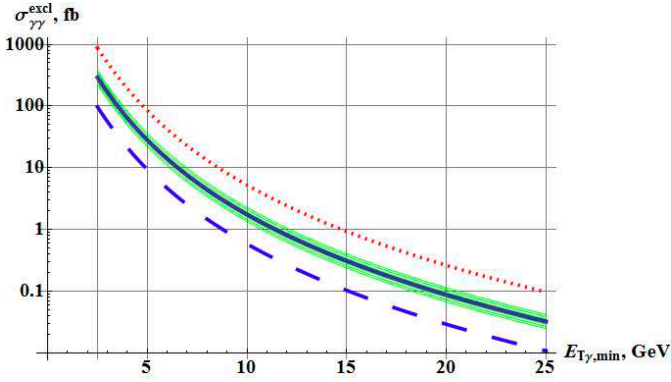


Fig. 10. CDF data on the exclusive di-gamma production cross-section [39] versus lower cut of $E_{T,\gamma}$ and prediction of the 3P-model. Solid curve corresponds to the value of $c_{gp}^{(3)}$ presented in (46) and obtained from fitting the HERA data on EVMP. Filled areas denote errors from $c_{gp}^{(3)}$. Results multiplied by 3 (dotted curve) and divided by 3 (dashed curve) are also shown.

to a factor $\frac{\times 3}{\div 3}$ (upper and lower curves are shown for the illustration of this fact in the Fig. 10) in the theoretical prediction. If we take into account this fact, CDF results [40],[41]

$$E_T > 5 \text{ GeV}, |\eta_\gamma| < 1 \implies \sigma_{\gamma\gamma}^{excl, CDF} < 410 \text{ fb}, \quad (86)$$

$$E_T > 2.5 \text{ GeV}, |\eta_\gamma| < 1 \\ \implies \sigma_{\gamma\gamma}^{excl, CDF} = 2.48^{+0.40}_{-0.35} (stat) \pm 0.40^{+0.40}_{-0.51} (syst) \text{ pb} \quad (87)$$

are in agreement with these predictions.

Our prediction for the $\chi_{c,0}$ production is

$$\left. \frac{d\sigma_{\chi_{c,0}}^{excl, th}}{dy} \right|_{y=0} = 15.9 \pm 4.1 \text{ nb} \quad (88)$$

and the CDF one [44] is

$$\left. \frac{d\sigma_{\chi_{c,0}}^{excl, CDF}}{dy} \right|_{y=0} = 76 \pm 10 (stat) \pm 10 (syst) \text{ nb}. \quad (89)$$

Theoretical prediction is about $3 \div 5$ times lower. As was mentioned above, the nonperturbative Pomeron-Pomeron and Reggeon-Reggeon fusion should be taken into account since this is the case of an intermediate invariant mass. For example, it was shown in [83],[84], that the nonperturbative contribution can be of the same order as the perturbative one. For more exact estimations we have to do similar calculations in our model.

Our approach can be checked once more in the CDF process of exclusive J/Ψ production $p + \bar{p} \rightarrow p + J/\Psi + \bar{p}$ which is governed by the photon-Pomeron fusion as in EVMP. We can obtain the cross-section as

$$\left. \frac{d\sigma_{J/\Psi}^{excl, th}}{dy} \right|_{y=0} = \mathcal{C}_{CDF} \times \sigma_{\gamma+p \rightarrow J/\Psi+p}(W_0) \\ = 3.51 \pm 0.45 \text{ nb}, \quad (90)$$

where

$$W_0 = \sqrt{m_{J/\Psi} \sqrt{s_{CDF}}} \simeq 78 \text{ GeV}, \quad \mathcal{C}_{CDF} \simeq 5.3 \times 10^{-5}$$

(see, for example, Ref. [82] for details of calculations). The CDF result [44] is

$$\left. \frac{d\sigma_{J/\Psi}^{excl, CDF}}{dy} \right|_{y=0} \\ = 3.92 \pm 0.25 (stat) \pm 0.52 (syst) \text{ nb}, \quad (91)$$

which is in a good agreement with the prediction. The prediction (90) does not depend much on the model (since the colliding energy W lies in the HERA interval), that is why it is shown only as an illustration.

Another “standard candle” is the di-hadron production. We have not considered this process yet, but one can find some results in [45],[85].

3.4 Standard candles for low invariant masses.

It is shown in the previous section that for invariant masses about several GeV (intermediate case) our model gives results systematically lower than the experimental data. It is naturally to assume that we have to take into account nonperturbative contributions to the Pomeron-Pomeron fusion. We can use, for example, NRQCD as in the case of EVMP, or the method considered in [84], where authors represent the Pomeron-Pomeron fusion in a similar way as the gamma-gamma fusion with different coupling (see Fig. 5b). We could use a similar representation in the EVMP process as depicted in Fig. 11a to obtain parameters of the model.

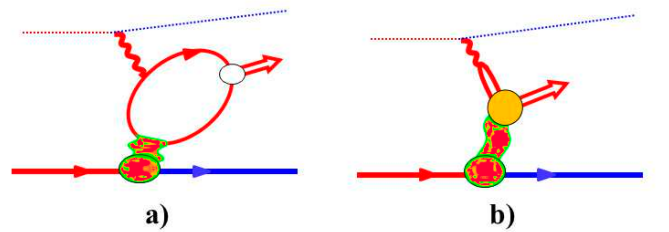


Fig. 11. Representations for EVMP processes with intermediate (a) $M \sim 3 - 10 \text{ GeV}$ and low (b) $M \sim 1 \text{ GeV}$ mass of vector meson.

The case of $M \sim 1 \text{ GeV}$ is more complicated, because we can not use any (even semi-perturbative like NRQCD) mechanism for calculations. We can only restrict ourselves by general representations for amplitudes like (80)-(83) and fit the data [33]-[37] with these distributions. The production of low mass resonances was considered in [59]. We can use this “standard candle” and also EVMP process with light vector mesons depicted in the Fig. 11b to obtain parameters of any nonperturbative approach. This

case is more convenient from the experimental point of view, since cross-sections are much larger than for high invariant masses. This is a powerful tool to look for new states like “glueballs” by the use of the azimuthal angular distributions [57],[58].

3.5 LHC predictions in the 3-Pomeron model.

In this section we collect some predictions of the 3-Pomeron model for the LHC.

The first prediction is devoted to the SM Higgs boson production

$$\sigma_{p+p \rightarrow p+H+p}(M_H = 125 \text{ GeV}) \simeq 0.55 \pm 0.15 \text{ fb}, \quad (92)$$

$$10^{-4} < \xi_{1,2} < 0.1, \quad 0.001 \text{ GeV}^2 < |t_{1,2}| < 1 \text{ GeV}^2. \quad (93)$$

This prediction is based on the EVMP HERA data, but the uncertainty in normalization on “standard candles” can be larger and reach a factor like $\frac{\times 3}{\div 3}$ [86].

Then we can calculate also di-jet and di-gamma production. Results are presented in Figs. 12,13. For the case of di-gamma production we can assume higher rate (as in CDF) due to nonperturbative effects. The latest LHC results [42] give the upper bound for the EDDE di-gamma production at $\sqrt{s} = 7 \text{ TeV}$

$$\begin{aligned} \sigma_{p+p \rightarrow p^* + \gamma\gamma + p^*} &< 1.18 \text{ pb}, \\ E_{T,\gamma} > 5.5 \text{ GeV}, \quad |\eta_\gamma| < 2.5, \end{aligned} \quad (94)$$

and no particles in the region $|\eta_\gamma| < 5.2$.

Now there are preliminary results from LHCb collaboration on exclusive $\chi_{c,0}$ and J/Ψ production at 7 TeV [43]:

$$\sigma_{\chi_{c,0}}^{excl, LHCb} = 160.9 \pm 78.8 \text{ nb}, \quad (95)$$

$$\sigma_{J/\Psi}^{excl, LHCb} = 81.9 \pm 18.3 \text{ nb}, \quad (96)$$

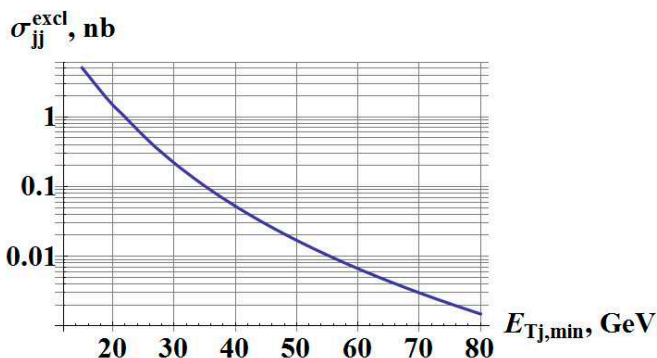


Fig. 12. EDDE di-jet production rate at LHC versus lower cut on the transverse energy of a jet for $\sqrt{s} = 8 \text{ TeV}$, $|\eta_{jet}| < 2.5$ plus cuts (93).

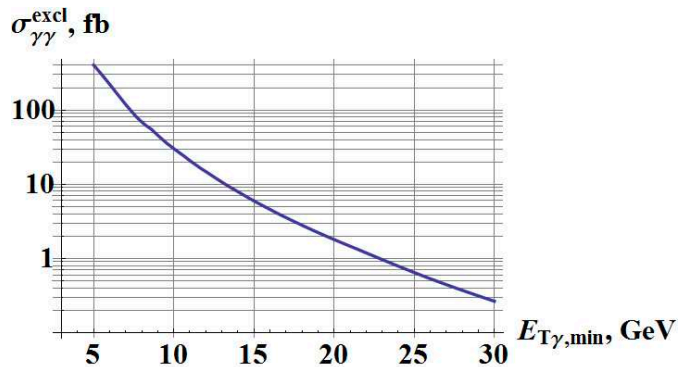


Fig. 13. EDDE di-gamma production rate at LHC versus lower cut on the transverse energy of a photon for $\sqrt{s} = 8 \text{ TeV}$, $|\eta_\gamma| < 2.5$ plus cuts (93).

Our predictions are

$$\left. \frac{d\sigma_{\chi_{c,0}}^{excl, th}}{dy} \right|_{y=0} = 20 \pm 5 \text{ nb}, \quad (97)$$

$$\sigma_{\chi_{c,0}}^{excl, th} = 212 \pm 53 \text{ nb}, \quad (98)$$

$$\begin{aligned} \left. \frac{d\sigma_{J/\Psi}^{excl, th}}{dy} \right|_{y=0} &= \mathcal{C}_{LHC} \times \sigma_{\gamma+p \rightarrow J/\Psi+p}(W_0) \\ &= 7.06 \pm 0.91 \text{ nb}, \end{aligned} \quad (99)$$

$$\sigma_{J/\Psi}^{excl, th} = 76.3 \pm 19.1 \text{ nb}, \quad (100)$$

where

$$W_0 = \sqrt{m_{J/\Psi} \sqrt{7000} \text{ GeV}} \simeq 147 \text{ GeV}, \quad \mathcal{C}_{LHC} \simeq 6.6 \times 10^{-5}.$$

These results are close to the experimental data.

Results for other interesting processes can be obtained by the use of master formulae (72),(73).

4 Conclusions and discussions.

In this article we consider the general framework for the exclusive double diffraction. In the present state of investigations we can describe it by the use of the prescription depicted in Fig. 5:

- for high invariant masses ($M \gg 1 \text{ GeV}$) we have to use a perturbative approach for the “bare” amplitude and calculate the gluon loop integral of the product of diffractive proton-gluon amplitudes T^D , gluon-gluon fusion vertex and Sudakov-like suppression factor (Fig. 5a);
- for intermediate invariant masses ($M \sim 3 \rightarrow 10 \text{ GeV}$ like in χ_c production) we can apply the NRQCD approach to the QQ -quarkonium vertex and the gamma-like approximation for a Pomeron [84];
- for low invariant masses ($M \sim 1 \text{ GeV}$) we have only the general representation (80)-(83) for the Pomeron-Pomeron fusion vertex. We can apply also some non-perturbative approaches like [57]-[24].

After the calculation of the “bare” amplitude we have to take into account different rescattering corrections (“soft survival probability”).

Let us note that in this paper we use the old version of 3-Pomeron model only as an example. After the comparison with the latest TOTEM data [87],[88] it shows discrepancy between the prediction and data points (as other popular models [89]), and we have to some update our approach to better fit the data.

The algorithm for EDDE calculations is far from an ideal one. This is because of our large gaps in understanding of the hadronic diffraction. There are different approaches at different scales. Also there are many models for diffractive amplitudes that are not always adequate (see [89] and references therein). This difficult task needs further intensive investigations, and EDDE is the most powerful tool in this scope of activity.

Appendix A

Here we collect basic expressions for gluon-gluon fusion partonic cross-sections of the type $g + g \rightarrow a + b$. Some of them can be found, for example, in [90] ($gg \rightarrow gg$, $gg \rightarrow Q\bar{Q}$) and [75] ($gg \rightarrow \gamma\gamma$).

$$\frac{d\hat{\sigma}_{gg \rightarrow gg}^{J_z=0}}{d\eta} = \frac{18\pi\alpha_s(M/2)^2 \cosh^2 \eta}{M^2}, \quad (101)$$

$$\frac{d\hat{\sigma}_{gg \rightarrow Q\bar{Q}}^{J_z=0}}{d\eta} = \frac{4\pi\alpha_s(M/2)^2 \cosh^2 \eta}{3M^2} \frac{m_Q^2}{M^2} \beta^2, \quad (102)$$

$$\beta = \sqrt{1 - \frac{4m_Q^2}{M^2}},$$

$$\frac{d\hat{\sigma}_{gg \rightarrow \gamma\gamma}^{J_z=0}}{d\eta} = \frac{121\alpha_e^2\alpha_s(M/2)^2}{324\pi M^2 \cosh^2 \eta} f_{\gamma\gamma}(\eta), \quad (103)$$

$$f_{\gamma\gamma}(\eta) = 1 + \left(1 - 2\eta \tanh \eta + \frac{\pi^2 + 4\eta^2}{4} (1 + \tanh^2 \eta)\right)^2,$$

where $\eta = (\eta_a - \eta_b)/2$, M is the invariant mass of the system, α_e and α_s are electromagnetic and strong couplings respectively, m_Q is the quark mass.

We use the following formulae for widths of resonances:

$$\Gamma_{H \rightarrow gg} = \frac{M_H^3}{4\pi} \frac{G_F}{\sqrt{2}} \left(\frac{\alpha_s(M_H/2)}{2\pi}\right)^2 \left|f_H\left(\frac{M_H^2}{4m_t^2}\right)\right|^2 K_H,$$

$$K_H \simeq 1 + \frac{\alpha_s(M_H/2)}{\pi} \left(\pi^2 + \frac{11}{2}\right) + 0.2,$$

$$f_H(x) = \frac{1}{x} \left(1 + \frac{1}{2} \left(1 - \frac{1}{x}\right) [L_+ + L_-]\right),$$

$$L_{\pm} = Li_2 \left(\frac{2}{1 \pm \sqrt{1 - \frac{1}{x}} \pm i0}\right), \quad (104)$$

$$\Gamma_{\chi_b \rightarrow gg} \simeq 354.4 \text{ keV} K_{\chi_b},$$

$$K_{\chi_b} \simeq 1 + \frac{9.8\alpha_s(m_{\chi_b}/2)}{\pi}, \quad m_{\chi_b} = 10.26 \text{ GeV}, \quad (105)$$

$$\Gamma_{\chi_c \rightarrow gg} \simeq 8.817 \text{ MeV} K_{\chi_c},$$

$$K_{\chi_c} \simeq 1.69, \quad m_{\chi_c} = 3.5 \text{ GeV} \quad (106)$$

where G_F is the Fermi constant and m_t is the top quark mass.

Appendix B

Here we present the calculation of the “soft survival probability” using (67) in the simple case, when the amplitude has the form

$$\mathcal{M} \sim \bar{\mathcal{M}} = e^{-B(\Delta_1^2 + \Delta_2^2)}. \quad (107)$$

When $y = 0$ we can take the above form of the amplitude. In this case

$$\int |\bar{\mathcal{M}}| d^2\Delta d^2\delta = \frac{\pi^2}{16B^2},$$

$$\Delta = \frac{\Delta_2 + \Delta_1}{2}, \quad \delta = \frac{\Delta_2 - \Delta_1}{2}, \quad (108)$$

and

$$\mathcal{M}^U \sim \bar{\mathcal{M}}^U = \int \frac{d^2\mathbf{q}}{(2\pi)^2} \frac{d^2\mathbf{q}'}{(2\pi)^2} d^2\mathbf{b} d^2\mathbf{b}' e^{i\mathbf{q}\mathbf{b} + i\mathbf{q}'\mathbf{b}'}$$

$$\times e^{-2B(\Delta^2 + \kappa^2) - \Omega(s,b) - \Omega(s',b')}, \quad (109)$$

where $\kappa = \mathbf{q} + \mathbf{q}' + \delta$, $b = |\mathbf{b}|$, $b' = |\mathbf{b}'|$,

$$\bar{\mathcal{M}}^U = e^{-2B\Delta^2} \int \frac{d^2\mathbf{b}}{2\pi} e^{-i\delta\mathbf{b} - \Omega(s,b) - \Omega(s',b)} \int \frac{d^2\mathbf{\kappa}}{2\pi} e^{i\mathbf{\kappa}\mathbf{b} - 2B\kappa^2}$$

$$= \frac{e^{-2B\Delta^2}}{4B} \int \frac{d^2\mathbf{b}}{2\pi} e^{-i\delta\mathbf{b} - \Omega(s,b) - \Omega(s',b) - b^2/(8B)}$$

$$= \frac{e^{-2B\Delta^2}}{4B} h(\delta), \quad (110)$$

where the function h is presented in (79). Finally we have

$$\int |\bar{\mathcal{M}}^U| d^2\Delta d^2\delta = \frac{\pi^2}{16B^2} \frac{1}{4B} \int_0^\infty |h(\delta)|^2 d\delta^2, \quad (111)$$

and

$$\langle S^2 \rangle \simeq \langle S^2 \rangle_{y=0} = \frac{\int |\bar{\mathcal{M}}^U| d^2\Delta d^2\delta}{\int |\bar{\mathcal{M}}| d^2\Delta d^2\delta}, \quad (112)$$

which leads to the expression (78). The accuracy of this approximation is about 1%.

Aknowledgements

Author thanks to V. A. Petrov, A. V. Prokudin, A. A. Godizov for useful discussions.

References

1. T.W. Kibble, Proc. Roy. Soc. **244**, 355 (1958)
2. A.A. Logunov, A.N. Tavkhelidze, Nucl. Phys. **8**, 374 (1958)
3. S.S. Gershtein, A.A. Logunov, *Growth Of Hadron Cross-sections And Its Possible Connection With Glueballs*, Sov. J. Nucl. Phys. **39**, 960 (1984) [Yad. Fiz. **39**, 1514 (1984)]
4. K.A. Ter-Martirosyan, Nucl. Phys. **68**, 591 (1964)
5. K.G. Boreskov, Yad. Fiz. **8**, 796 (1968)
6. A. Actor, *Characteristics of double-pomeron exchange*, Ann. of Phys. **109**, 317 (1977)
7. J. Pumplin, F.S. Henyey, *Double pomeron exchange in the reaction $pp \rightarrow pp\pi^+\pi^-$* , Nucl. Phys. B **117**, 377 (1976)
8. A. Bialas, P.V. Landshoff, *Higgs production in $p p$ collisions by double pomeron exchange* Phys. Lett. B **256**, 540 (1991)
9. B.R. Desai, B.C. Shen, M. Jacob, *Double pomeron exchange in high-energy pp collisions*, Nucl. Phys. B **142**, 258 (1978)
10. L.A. Harland-Lang, V.A. Khoze, M.G. Ryskin, W.J. Stirling, *The Phenomenology of Central Exclusive Production at Hadron Colliders*, Eur. Phys. J. C **72**, 2110 (2012)
11. V.A. Khoze, A.D. Martin, M.G. Ryskin, *New Physics with Tagged Forward Protons at the LHC*, Frascati Phys. Ser. **44**, 147 (2007)
12. V.A. Khoze, A.B. Kaidalov, A.D. Martin, M.G. Ryskin, *Diffractive processes as a tool for searching for new physics*, DCPT-05-72, IPPP-05-36, arXiv: hep-ph/0507040.
13. L.A. Harland-Lang, V.A. Khoze, M.G. Ryskin, W.J. Stirling *Standard candle central exclusive processes at the Tevatron and LHC*, Eur. Phys. J. C **69**, 179 (2010)
14. V.A. Petrov, R.A. Ryutin, *Exclusive double diffractive events: Menu for LHC*, JHEP **0408**, 013 (2004)
15. V.A. Petrov, R.A. Ryutin, *Patterns of the exclusive double diffraction*, J. Phys. G **35**, 065004 (2008)
16. V.A. Petrov, R.A. Ryutin, *Exclusive double diffractive Higgs boson production at LHC*, Eur. Phys. J. C **36**, 509 (2004)
17. J.R. Cudell, A. Dechambre, O.F. Hernandez, *Higgs Central Exclusive Production*, Phys. Lett. B **706**, 333 (2012)
18. M.G. Albrow, T.D. Coughlin, J.R. Forshaw, *Central Exclusive Particle Production at High Energy Hadron Colliders*, Prog. Part. Nucl. Phys. **65**, 149 (2010)
19. E.V. Shuryak, I. Zahed, *Semiclassical double pomeron production of glueballs and eta-prime*, Phys. Rev. D **68**, 034001 (2003)
20. D. Kharzeev, E. Levin, *Soft double diffractive Higgs production at hadron colliders*, Phys. Rev. D **63**, 073004 (2001)
21. J. Ellis, D. Kharzeev, *The Glueball filter in central production and broken scale invariance*, Preprint CERN-TH-98-349, arXiv: hep-ph/9811222.
22. N.I. Kochelev, *Unusual properties of the central production of glueballs and instantons*, arXiv: hep-ph/9902203.
23. R.C. Brower, M. Djuric, C.-I. Tan, *Diffractive Higgs Production by AdS Pomeron Fusion*, JHEP **1209**, 097 (2012)
24. M.V.T. Machado, *Investigating the central diffractive $f_0(980)$ and $f_2(1270)$ meson production at the LHC*, Phys. Rev. D **86**, 014029 (2012)
25. B.Z. Kopeliovich, I. Schmidt, *Higgs diffractive production*, Nucl. Phys. A **782**, 118 (2007)
26. A. Bzdak, *Exclusive Higgs and dijet production by double pomeron exchange: The CDF upper limits*, Phys. Lett. B **615**, 240 (2005)
27. E. Gotsman, H. Kowalski, E. Levin, U. Maor, A. Prygarin, *Survival probability for diffractive dijet production at the LHC*, Eur. Phys. J. C **47**, 655 (2006)
28. S.M. Troshin, N.E. Tyurin, *Reflective scattering effects in double-pomeron exchange processes*, Mod. Phys. Lett. A **23**, 169 (2008)
29. R. Enberg, G. Ingelman, N. Timneanu, *Soft color interactions and diffractive Higgs production*, Eur. Phys. J. C **33**, S542 (2004)
30. C.P. Herzog, S. Paik, M.J. Strassler, E.G. Thompson, *Holographic Double Diffractive Scattering*, JHEP **0808**, 010 (2008)
31. D.M. Chew, *Search for experimental evidence on exclusive double-pomeron exchange*, Nucl. Phys. **82**, 422 (1974)
32. Yu.D. Prokoshkin, *The experiment to study the gluon interactions and glueball production in the central region of hadron collisions at UNK energies (2-3 TeV)*, IFVE-85-32 (1985)
33. WA102 Collaboration, *A Study of pseudoscalar states produced centrally in $p p$ interactions at 450 GeV/c*, Phys. Lett. B **427**, 398 (1998)
34. WA102 Collaboration, *Experimental evidence for a vector like behavior of Pomeron exchange*, Phys. Lett. B **467**, 165 (1999)
35. WA102 Collaboration, *A Study of the $f_0(1370)$, $f_0(1500)$, $f_0(2000)$ and $f_2(1950)$ observed in the centrally produced 4π final states*, Phys. Lett. B **474**, 423 (2000)
36. WA102 Collaboration, *A Coupled channel analysis of the centrally produced $K^+ K^-$ and $\pi^+ \pi^-$ final states in $p p$ interactions at 450 GeV/c*, Phys. Lett. B **462**, 462 (1999)
37. A. Kirk, *Resonance production in central $p p$ collisions at the CERN Omega spectrometer*, Phys. Lett. B **489**, 29 (2000)
38. K. Goulios (CDF II Collaboration), *Diffraction Results from CDF*, arXiv:1204.5241 [hep-ex]
39. T. Aaltonen et al. (CDF Collaboration), *Observation of Exclusive Dijet Production at the Fermilab Tevatron $p\bar{p}$ Collider*, Phys. Rev. D **77**, 052004 (2008)
40. T. Aaltonen et al. (CDF Collaboration), *Observation of Exclusive Gamma Gamma Production in $p\bar{p}$ Collisions at $\sqrt{s} = 1.96$ TeV*, Phys. Rev. Lett. **108**, 081801 (2012)
41. T. Aaltonen et al. (CDF Collaboration), *Search for exclusive $\gamma\gamma$ production in hadron-hadron collisions*, Phys. Rev. Lett. **99**, 242002 (2007)
42. G.A. Alves et al. (for the CMS Collaboration), *Search for central exclusive gamma pair production and observation of central exclusive electron pair production in pp collisions at $\sqrt{s} = 7$ TeV*, CMS-PAS-FWD-11-004, CERN-PH-EP-2012-246 (2012), accepted for publication in JHEP.
43. D. Moran, *Central Exclusive Production with Dimuon Final States at LHCb*, CERN-THESIS-2011-209 (2011)
44. T. Aaltonen et al. (CDF Collaboration), *Observation of exclusive charmonium production and $\gamma\gamma \rightarrow \mu^+\mu^-$ in p anti- p collisions at $\sqrt{s} = 1.96$ TeV*, Phys. Rev. Lett. **102**, 242001 (2009)
45. L.A. Harland-Lang, V.A. Khoze, M.G. Ryskin, W.J. Stirling, *Central exclusive meson pair production in the perturbative regime at hadron colliders*, Eur. Phys. J. C **71**, 1714 (2011)
46. V.A. Petrov, A.V. Prokudin, R.A. Ryutin, *From the exclusive photoproduction of heavy quarkonia at HERA to the EDDE at Tevatron and LHC*, Czech. J. Phys. **55**, 17 (2005)
47. V.A. Petrov, A.V. Prokudin, *The First three pomerons....*, Eur. Phys. J. C **23**, 135 (2002)
48. J.D. Bjorken, *Rapidity gaps and jets as a new-physics signature in very-high-energy hadron-hadron collisions*, Phys. Rev. D **47**, 101 (1993)

49. F. Abe et al. (CDF Collaboration), *Observation of rapidity gaps in $\bar{p}p$ collisions at 1.8 TeV*, Phys. Rev. Lett. **74**, 855 (1995)
50. M.G. Albrow, A. Rostovtsev, *Searching for the Higgs at hadron colliders using the missing mass method*, FERMILAB-PUB-00-173 (2000), arXiv: hep-ph/0009336 [hep-ph]
51. J. Pumplin, *Two gluon exchange model predictions for double pomeron jet production*, Phys. Rev. D **52**, 1477 (1995)
52. V.A. Khoze, A.D. Martin, M.G. Ryskin, *Double diffractive processes in high resolution missing mass experiments at the Tevatron*, Eur. Phys. J. C **19**, 477 (2001); Erratum-ibid. C **20**, 599 (2001)
53. A. De Roeck, V.A. Khoze, A.D. Martin, R. Orava, M.G. Ryskin, *Ways to detect a light Higgs boson at the LHC*, Eur. Phys. J. C **25**, 391 (2002)
54. J.G. Rushbrooke, B.R. Webber, *Spin-parity analysis of $\pi\pi$ systems produced in $pp \rightarrow pp\pi^+\pi^-$ and the question of double pomeron exchange*, Nucl. Phys. B. **88**, 145 (1975)
55. A.B. Kaidalov, V.A. Khoze, A.D. Martin, M.G. Ryskin, *Central exclusive diffractive production as a spin-parity analyser: From Hadrons to Higgs*, Eur. Phys. J. C **31**, 387 (2003)
56. V.A. Khoze, A.D. Martin, M.G. Ryskin, *Physics with tagged forward protons at the LHC*, Eur. Phys. J. C **24**, 581 (2002)
57. F.E. Close, G.A. Schuller, *Central production of mesons: Exotic states versus pomeron structure*, Phys. Lett. B **458**, 127 (1999)
58. F.E. Close, G.A. Schuller, *Evidence that the pomeron transforms as a nonconserved vector current*, Phys. Lett. B **464**, 279 (1999)
59. V.A. Petrov, R.A. Ryutin, A.E. Sobol, J.-P. Guillaud, *Azimuthal angular distributions in EDDE as spin-parity analyser and glueball filter for LHC*, JHEP **0506**, 007 (2005)
60. K. Eggert, *The TOTEM/CMS forward experiment at the LHC*, Nucl. Phys. Proc. Suppl. **122**, 447 (2003)
61. M.G. Albrow et al. (FP420 R&D Collaboration), *The FP420 R&D Project: Higgs and New Physics with forward protons at the LHC*, JINST **4**, T10001 (2009)
62. M. Albrow et al. (USCMS Collaboration), *Forward Physics with Rapidity Gaps at the LHC*, JINST **4**, P10001 (2009)
63. M. Tasevsky (for the ATLAS Collaboration), *Diffractive and central exclusive production at ATLAS*, AIP Conf. Proc. **1350**, 164 (2010)
64. V.A. Khoze, F. Krauss, A.D. Martin, M.G. Ryskin, K.C. Zapp, *Diffractive and correlations at the LHC: Definitions and observables*, Eur. Phys. J. C **69**, 85 (2010)
65. J.H. Lee (for the STAR Collaboration), *Physics Program with Tagged Forward Protons at STAR/RHIC*, arXiv:0908.4552 [hep-ex]
66. J.H. Lee (for the STAR Collaboration), *Diffractive physics program with tagged forward protons at STAR/RHIC*, PoS **DIS2010**, 076 (2010)
67. W. Guryn (for the STAR Collaboration), *Central Production with Tagged Forward Protons and the Star Detector at RHIC*, arXiv:0808.3961 [nucl-ex]
68. W. Guryn, *Physics with tagged forward protons at RHIC*, Acta Phys. Polon. B **40**, 1897 (2009)
69. S. Chekanov et al. (ZEUS Collaboration), *Exclusive photoproduction of J/ψ mesons at HERA*, Eur. Phys. J. C **24**, 345 (2002)
70. S. Chekanov et al. (ZEUS Collaboration), *Exclusive photoproduction of epsilon mesons at HERA*, Phys. Lett. B **680**, 4 (2009)
71. J. Breitweg et al. (ZEUS Collaboration), *Measurement of elastic Upsilon photoproduction at HERA*, Phys. Lett. B **437**, 432 (1998)
72. M. Derrick et al. (ZEUS Collaboration), *Measurement of elastic omega photoproduction at HERA*, Z. Phys. C **73**, 73 (1996)
73. J. Breitweg et al. (ZEUS Collaboration), *Elastic and proton dissociative ρ_0 photoproduction at HERA*, Eur. Phys. J. C **2**, 247 (1998)
74. M. Derrick et al. (ZEUS Collaboration), *Measurement of elastic ϕ photoproduction at HERA*, Phys. Lett. B **377**, 259 (1996)
75. R. Gastmans, T.T. Wu, *The Ubiquitous Photon: Helicity Method For QED And QCD*, (Oxford, UK: Clarendon, 1990), 648 p.
76. C.S. Kim, E. Mirkes, *Testing J/ψ production and decay properties in hadronic collisions*, Phys. Rev. D **51**, 3340 (1995)
77. M. Kramer, *Quarkonium production at high-energy colliders*, Prog. Part. Nucl. Phys. **47**, 141 (2001)
78. C.G. Callan, D.J. Gross, *High-energy electroproduction and the constitution of the electric current*, Phys. Rev. Lett. **22**, 156 (1969)
79. C.G. Callan, D.J. Gross, *Crucial Test of a Theory of Currents*, Phys. Rev. Lett. **21**, 311 (1968)
80. V.A. Khoze, A.D. Martin, M.G. Ryskin, *Can the Higgs be seen in rapidity gap events at the Tevatron or the LHC?*, Eur. Phys. J. C **14**, 525 (2000) 525; *ibid.* C **21**, 99 (2001)
81. A. Berera and J.C. Collins, *Double pomeron jet cross-sections*, Nucl. Phys. B **474**, 183 (1996)
82. L. Motyka, G. Watt, *Exclusive photoproduction at the Tevatron and CERN LHC within the dipole picture*, Phys. Rev. D **78**, 014023 (2008)
83. L.A. Harland-Lang, V.A. Khoze, M.G. Ryskin, W.J. Stirling, *Central exclusive χ_c meson production at the Tevatron revisited*, Eur. Phys. J. C **65**, 433 (2010)
84. V.A. Khoze, A.D. Martin, M.G. Ryskin, W.J. Stirling, *Double diffractive chi meson production at the hadron colliders*, Eur. Phys. J. C **35**, 211 (2004)
85. R. Staszewski, P. Lebiedowicz, M. Trzebinski, J. Chwastowski, A. Szczurek, *Exclusive $\pi^+\pi^+$ Production at the LHC with Forward Proton Tagging*, Acta Phys. Polon. B **42**, 1861 (2011)
86. A.B. Kaidalov, V.A. Khoze, A.D. Martin, M.G. Ryskin, *Extending the study of the Higgs sector at the LHC by proton tagging*, Eur. Phys. J. C **33**, 261 (2004)
87. The TOTEM Collaboration, *Proton-proton elastic scattering at the LHC energy of $\sqrt{s} = 7$ TeV*, Europhys. Lett. **95**, 41001 (2011)
88. The TOTEM Collaboration, *First measurement of the total proton-proton cross section at the LHC energy of $\sqrt{s} = 7$ TeV*, Europhys. Lett. **96**, 21002 (2011)
89. A.A. Godizov, *Models of elastic diffractive scattering to falsify at the LHC*, PoS **IHEP-LHC-2011**, 005 (2012); arXiv:1203.6013 [hep-ph]
90. V.A. Khoze, A.D. Martin, M.G. Ryskin, *Prospects for new physics observations in diffractive processes at the LHC and Tevatron*, Eur. Phys. J. C **23**, 311 (2002)

